LANGMUIR

Article

pubs.acs.org/Langmuir

Formation and Properties of Vesicles from Cyclic Amphiphilic PS–PEO Block Copolymers

Eisuke Baba,[†,§] Toshiaki Yatsunami,[†] Yasuyuki Tezuka,[†] and Takuya Yamamoto*[,†,‡]

[†]Department of Organic and Polymeric Materials, Tokyo Institute of Technology, O-okayama, Meguro-ku, Tokyo 152−8552, Japan

[‡]Division of Applied Chemistry, Faculty of Engineering, Hokkaido University, Sapporo, Hokkaido 060−8628, Japan

Supporting Information

ABSTRACT: Linear polystyrene−poly(ethylene oxide)−polystyrene (PS−PEO−PS) block copolymers and corresponding cyclized PS−PEO counterparts with three different PS molecular weights were synthesized and self-assembled to investigate the effects arising from the topology. Linear PS_5−PEO_{45}−PS_5 (**L1**) and cyclic PS_{10}−PEO_{45} (**C1**) formed micelles. As previously reported for poly(*n*-butyl acrylate) and PEO block copolymers, the micelles from **C1** showed more than 30 °C higher phase transition temperature (cloud point, T_c) than those from **L1**. Linear PS_{10}−PEO_{45}−PS_{10} (**L2**) and cyclic PS_{20}−PEO_{45} (**C2**) resulted in the formation of a structure called large compound micelles. Self-assembly of linear PS_{40}−PEO_{48}−PS_{40} (**L3**) and cyclic PS_{86}−PEO_{48} (**C3**) lead to the formation of vesicles. The vesicles were characterized by TEM, DLS, and SLS. Remarkably, the vesicles from **L3** (T_c = 69, 59, and 48 °C in the presence of 1, 5, and 10 wt % of NaCl, respectively) were found to be somewhat more thermally stable than those from **C3** (T_c = 62, 52, and 43 °C in the presence of 1, 5, and 10 wt % of NaCl, respectively). This trend of the thermal stability was counterintuitively opposed to the case of the micelles. Moreover, T_c of the vesicles was controlled by the ratio of **L3** and **C3**.

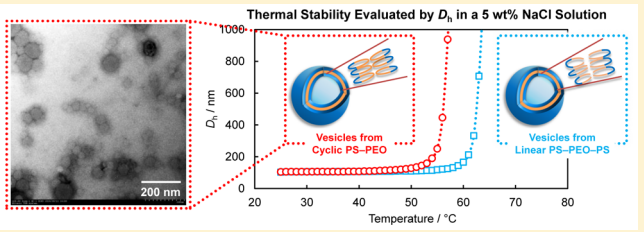

INTRODUCTION

Cyclic polymers show unique properties and functions, which are called "topology effects", due to the absence of their chain ends and the restricted conformation, in comparison with their linear or branched counterparts.[1] For example, topology effects were found in the basic properties of polymers such as melting,[2] crystallization,[3−5] diffusion,[6] and rheology[7] as well as in gels[8] and degradable polymers.[9] Moreover, cyclic polymers were even applied to potential drug delivery systems.[10,11] It is conceivable that cyclic polymers may provide further novel properties and functions in their self-assembled structures.[12] These topology effects can be a novel factor in materials development, because they improve or change material properties and stabilities without alteration of the chemical structure, composition, or molecular weight. Therefore, cyclic polymers have cultivated curiosity, and the synthesis and self-assembly of cyclic polymers including cyclic block copolymers have been greatly developed in the past decade.[13−17]

Cyclic molecules and their self-assembled structures are also exploited in nature, typically in DNA,[18] polypeptides,[19] and polysaccharides.[20] Significant functionalities arise from this unique shape, especially in relation to the stability of such structures. Thermophilic archaea, living in high-temperature environment such as hot springs and submarine volcanoes, have cyclic lipids in their cell membranes.[21,22] Their cell membranes are considered to enable them to adapt to such extreme environments by exploiting the topology effect. Therefore, cyclic amphiphilic block copolymers are expected to exhibit excellent tolerance to extreme conditions through their self-assembled nanostructures. Indeed, in recent years, we reported on micelles formed from synthesized cyclic amphiphilic block copolymers (i.e., a series of poly(alkyl acrylate)−poly(ethylene oxide)) exhibiting significantly enhanced thermal stability in comparison to micelles formed from their linear counterparts.[23,24] This finding is regarded as the first example of amplified topology effects by a synthetic cyclic polymer upon self-assembly.

In this study, we focused on the formation of vesicles (Figure 1), which have a bilayer structure, resembling to the cell membrane of thermophilic archaea. We expected that vesicles formed from the synthesized cyclic amphiphilic block copolymers show excellent thermal stability in comparison to vesicles formed from their linear counterparts. In order to construct vesicles, the volume fractions of the hydrophilic and hydrophobic segments were needed to be properly tuned.[25] Thus, the previously reported atom transfer radical polymerization−ring-closing metathesis (ATRP−RCM) method was applied to provide a variety of cyclic block copolymers having a programmed combination of the segment components with narrow PDIs.[26] This method was also used in the synthesis of a 8-shaped polymer, demonstrating the versatility in the construction of cyclic topologies.[27] Moreover, amphiphilic

Received: August 24, 2016
Revised: September 8, 2016
Published: September 13, 2016

DOI: 10.1021/acs.langmuir.6b03148
Langmuir 2016, 32, 10344−10349

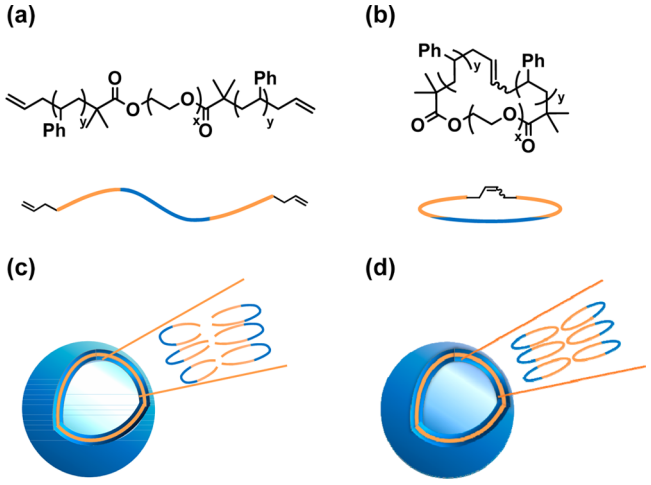

Figure 1. Chemical structures of (a) linear (**L1**, **L2**, and **L3**) and (b) cyclic (**C1**, **C2**, and **C3**) amphiphilic PS–PEO bock copolymers and schematic representation of vesicles from (c) **L3** and (d) **C3**.

block copolymers comprised of polystyrene segments are of importance because self-assembled micellar structures, vesicles, and other complex aggregates formed from linear PS–PEO block copolymers have been extensively studied.[28,29] Therefore, relevant cyclic PS–PEO counterparts would warrant the formation of vesicles and provide unique opportunities to reveal topology effects upon self-assembly. Furthermore, polystyrene is one of the most common and utilized polymer segments in various fields. Having polystyrene as the hydrophobic segments in the amphiphilic block copolymers should expand the generality of the chemistry of cyclic polymers.

EXPERIMENTAL SECTION

Reagents. Styrene (99%, Nacalai Tesque, Inc.) was purified through an alumina column. CH_2Cl_2 (99%, Kanto Chemical Co., Inc.) was distilled from CaH_2 before use. A PEO macroinitiator with 2-bromoisobutyryl end groups (M_n(NMR) = 2300) was prepared by esterification of hydroxy-terminated PEO (M_n = 2000, Aldrich) with 2-bromoisobutyryl bromide (98%, Aldrich) and triethylamine (99%, Kanto Chemical Co., Inc.) according to the previously reported procedure.[30,31]

Linear PS–PEO–PS (**L1**, **L2**, and **L3**) (M_n = 500–2000–500, 1100–2000–1100, 4100–2100–4100) and cyclic PS–PEO (**C1**, **C2**, and **C3**) (M_n = 1000–2000, 2100–2000, 8900–2100) were synthesized using the method described in the previous report.[26]

TEM. A drop of an aqueous solution containing self-assembled structures was placed on a carbon-coated copper grid and blown away with an air blower. TEM observations were carried out on a Hitachi H-7650 microscope operating at 80 kV.

Turbidity of Micellar Solutions. The transmittance of a micellar solution was measured at 600 nm on a JASCO V-670 spectrophotometer with a stepwise temperature increase from 20 to 80 °C. The temperature was equilibrated for 1 min before measurements.

DLS and SLS. DLS and SLS measurements were performed on a Malvern Zetasizer Nano spectrometer equipped with a He–Ne laser (λ = 532 nm). The light scattering signal was obtained at a fixed angle of 173°. D_h distributions were determined by the non-negative least-squares[32−35] fit to the autocorrelation functions. *Z*-average diameters were calculated from the second-order cumulant of the autocorrelation functions. N_{agg} and A_2 were determined by Debye plots using the Zimm equation with polymer concentrations of 0.10, 0.075, 0.050, 0.020 mg/mL for **L3** and 0.10, 0.075, 0.050, 0.030, 0.020 mg/mL for **C3**. Specimens were filtered off with a 0.45-μm membrane filter before measurements.

Self-Assembly of PS_5–PEO_{45}–PS_5 (L1) and Cyclic PS_{10}–PEO_{45} (C1). Aqueous micellar solutions of **L1** and **C1** were prepared according to literature.[23] Thus, distilled water (10 mL) was added to a vigorously stirred THF solution of **L1** or **C1** (5.0 mg/mL, 2.0 mL) at a drop rate of one drop per 5 s. THF was removed under reduced pressure, and distilled water was added to a total volume of 10 mL to give a 1.0 mg/mL micellar solution. The solution was further diluted to 0.33 mg/mL.

Self-Assembly of PS_{10}–PEO_{45}–PS_{10} (L2) and Cyclic PS_{20}–PEO_{45} (C2). Aqueous large compound micellar solutions of **L2** and **C2** were prepared according to literature.[36,37] Thus, distilled water (10 mL) was added to a vigorously stirred THF solution of **L2** or **C2** (10 mg/mL, 1.0 mL) at a drop rate of one drop per 5 s. The THF/water solution was dialyzed against water for 3 days.

Self-Assembly of PS_{40}–PEO_{48}–PS_{40} (L3) and Cyclic PS_{86}–PEO_{48} (C3). A THF solution of **L3** or **C3** (1.0 mg/mL, 1.0 mL) was added at a drop rate of one drop per 5 s to distilled water (10 mL), which was stirred at a specific rate (500, 900, 700, and 1100 rpm). The THF/water solution was dialyzed against water for 5 days.

RESULTS AND DISCUSSION

Linear and cyclic PS–PEO block copolymers with three different volume fractions (Table 1) were prepared by the ATRP–RCM cyclization method using PEO with molecular weight of 2 kDa (Figures S1 and S2).[26] Block copolymers with various molecular weights of the PS segments were synthesized in order to control the hydrophobic/hydrophilic volume ratio. According to the critical packing parameter (CPP) theory,[38,39] this ratio copolymer determines the morphology of the self-assembly such as micelles, wormlike micelles, and vesicles.[40,41] The self-assembly of linear PS_5–PEO_{45}–PS_5 (**L1**) and cyclic PS_{10}–PEO_{45} (**C1**) was performed by dissolving a block copolymer (10 mg) in THF (2.0 mL) and adding water (10 mL) dropwise to the vigorously stirred THF solution. THF was removed under reduced pressure to give an aqueous solution of the block copolymer, and water was added to adjust the concentration to 1.0 and 0.33 mg/mL. The hydrodynamic diameter (D_h) of both self-assembled structures formed from **L1** and **C1** was determined to be 10 nm with a polydispersity index of 0.56 and 0.54, respectively, by dynamic light scattering (DLS) shown in Figure S3. This suggests the conversion of the polymer topology from linear to cyclic did not cause distinctive changes in their D_h.[23,24] The thermal stability of the micelles were determined by the turbidity of the micellar solutions and D_h by DLS upon raising the temperature. The transmittance of the micellar solution of **L1** started to decrease at 33 °C, indicating the collapse of the micelles and formation of larger agglomerates (Figure S4). In sharp contrast, the micellar

Table 1. Properties of the Linear and Cyclic PS–PEO Amphiphilic Block Copolymers and Their Self-Assembled Structures

	chemical structure	M_n(NMR)	self-assembled structure
L1	linear PS_5–PEO_{45}–PS_5	500–2000–500	micelle
C1	cyclic PS_{10}–PEO_{45}	1000–2000	micelle
L2	linear PS_{10}–PEO_{45}–PS_{10}	1100–2000–1100	large compound micelle
C2	cyclic PS_{20}–PEO_{45}	2100–2000	large compound micelle
L3	linear PS_{40}–PEO_{48}–PS_{40}	4100–2100–4100	vesicle
C3	cyclic PS_{86}–PEO_{48}	8900–2100	vesicle

DOI: 10.1021/acs.langmuir.6b03148
Langmuir 2016, 32, 10344–10349

solution of **C1** did not show significant reduction in transmittance until 64 °C. DLS showed a sharp increase in the *z*-average diameter at corresponding T_c. Thus, the phase transition temperature, or cloud point (T_c), increased by more than 30 °C through the topological conversion of the polymeric component, where T_c of the micellar solutions was defined by the temperature, at which the transmittance becomes 99% of the initial value. This process was reversible, allowing for the formation of micelles or agglomerates by cooling or heating, respectively (Figure S5).

The self-assembly of linear PS_{10}–PEO_{45}–PS_{10} (**L2**) and cyclic PS_{20}–PEO_{45} (**C2**) shown in Table 1 was performed by adding water to a THF solution of a copolymer, followed by dialysis. The morphology of the polymer aggregates was observed by TEM. Figure S6 shows agglomerated structures with a diameter from 100 nm to 1 μm for **L2** and from 100 to 500 nm for **C2**. DLS demonstrated that the formation of particles that have D_h of 700 and 500 nm, respectively (Figure S7). The structures were likely large compound micelles,[25] suggesting that the volume fractions of the block copolymers was not appropriate for the formation of either micelles or vesicles.

The molecular weight of the PS segment was further increased to change the volume fractions (**L3**, PS_{40}–PEO_{48}–PS_{40}; **C3**, PS_{86}–PEO_{48}) as shown in Table 1. We first attempted to self-assemble by the same methods above. However, precipitate formed upon removing THF from the aqueous solution under reduced pressure. After all the efforts to investigate the conditions for the self-assembly, dripping a THF solution of a polymer to agitating water at a specific rate and following dialysis was found to be successful. Thus, 1.0 mg/mL of a THF solution containing 2.0 mg of a copolymer was added dropwise to water (20 mL), which was being agitated at the rate of 500 rpm. The THF/water solution was dialyzed against water for 5 days. The resulting solution was pale blue due to the scattering of the particular wavelengths by the formed particles (Figure S8). The morphology of self-assembled structures was observed by TEM (Figure 2). The structure was confirmed to

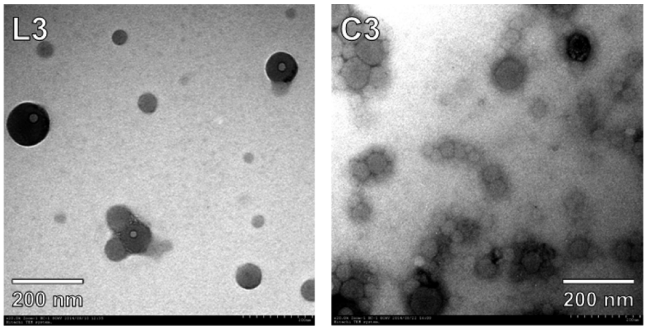

Figure 2. TEM images of air-blown and vacuum-dried aqueous vesicular solutions of **L3** (left) and **C3** (right) formed at the agitation rate of water at 500 rpm upon addition of a THF solution of a copolymer.

be vesicles by observing a void likely enveloped with a bilayer. Torn bilayers can be observed in Figure 2, left, leaving a hole on the vesicles. This was presumably caused by the evaporation of encapsulated water under vacuum conditions. The diameter of the vesicles were 30–120 nm for **L3** (Figure 2, left) and 30–100 nm for **C3** (Figure 2, right). By DLS, the D_h distribution of the vesicles formed from **L3** and **C3** had a peak at 109 and 112 nm (Figure 3, top), respectively, through the above procedure. Here, the effects of the agitation rate of water at the dripping of

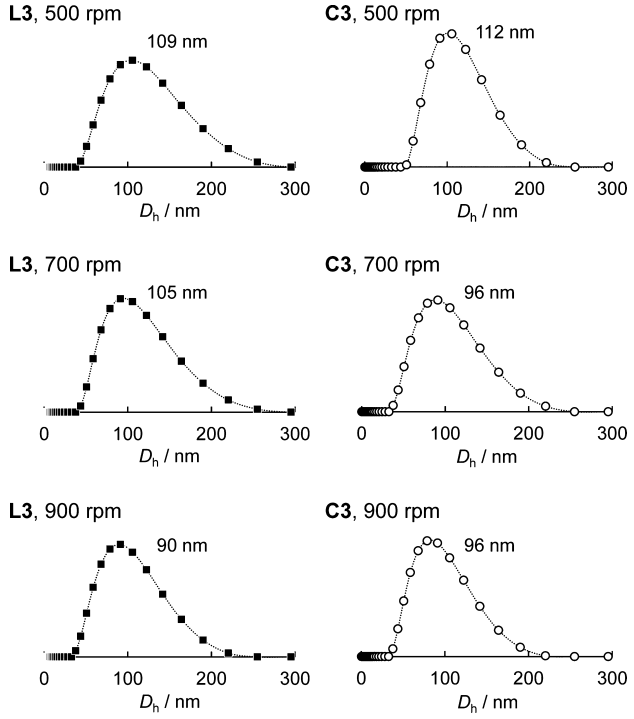

Figure 3. D_h distributions by number for vesicular solutions of **L3** (left) and **C3** (right) formed at the agitation rate of water at 500 (top), 700 (middle), and 900 rpm (bottom) upon addition of a THF solution of a copolymer.[46] At the agitation rate of water at 1100 rpm, a precipitate formed from both **L3** and **C3**.

a THF solution of a copolymer were investigated. The agitation rate was increased to 700 and 900 rpm, and D_h of the vesicles decreased to 105 and 90 nm for **L3** and 96 and 96 nm for **C3** (Figure 3, middle and bottom, respectively). This suggests that the stronger shear during agitation caused smaller size of the vesicles. When the agitation rate was further increased to 1100 rpm, a precipitate formed. Hence, too strong shear likely disturbed the formation of the bilayer structure. By means of SLS, the weight-average molecular weight of the vesicles formed at 500 rpm was determined to be 85 and 95 MDa for **L3** and **C3**, respectively (Figure S9). Based on the molecular weight of the block copolymers, the aggregation number (N_{agg}) was calculated to be 8300 and 8600, respectively. Considering the comparable size recorded for both vesicles by DLS (**L3**, 109; **C3**, 112 nm), the density of the bilayer was not significantly altered. The second virial coefficient (A_2), which accounts for the strength of the interaction between the dispersed particles in a solvent, was determined to be 6.4×10^{-5} mL·mol/g^2 for **L3** and 7.4×10^{-5} mL·mol/g^2 for **C3**. This trend was same as that for micelles.[23] This result suggests that the repulsive interaction between the vesicles formed from **C3** was stronger than those from **L3**, which could be due to the absence and presence, respectively, of the intervesicular bridging just like micelles.[42−44]

The thermal stability of the vesicles was investigated by temperature-dependent DLS measurements. Both vesicles from **L3** and **C3** were stable from 25 to 75 °C in water, and no difference was observed by this experiment. Thus, NaCl (1, 5, and 10 wt %) was added to the aqueous vesicular solutions to

DOI: 10.1021/acs.langmuir.6b03148
Langmuir 2016, 32, 10344−10349

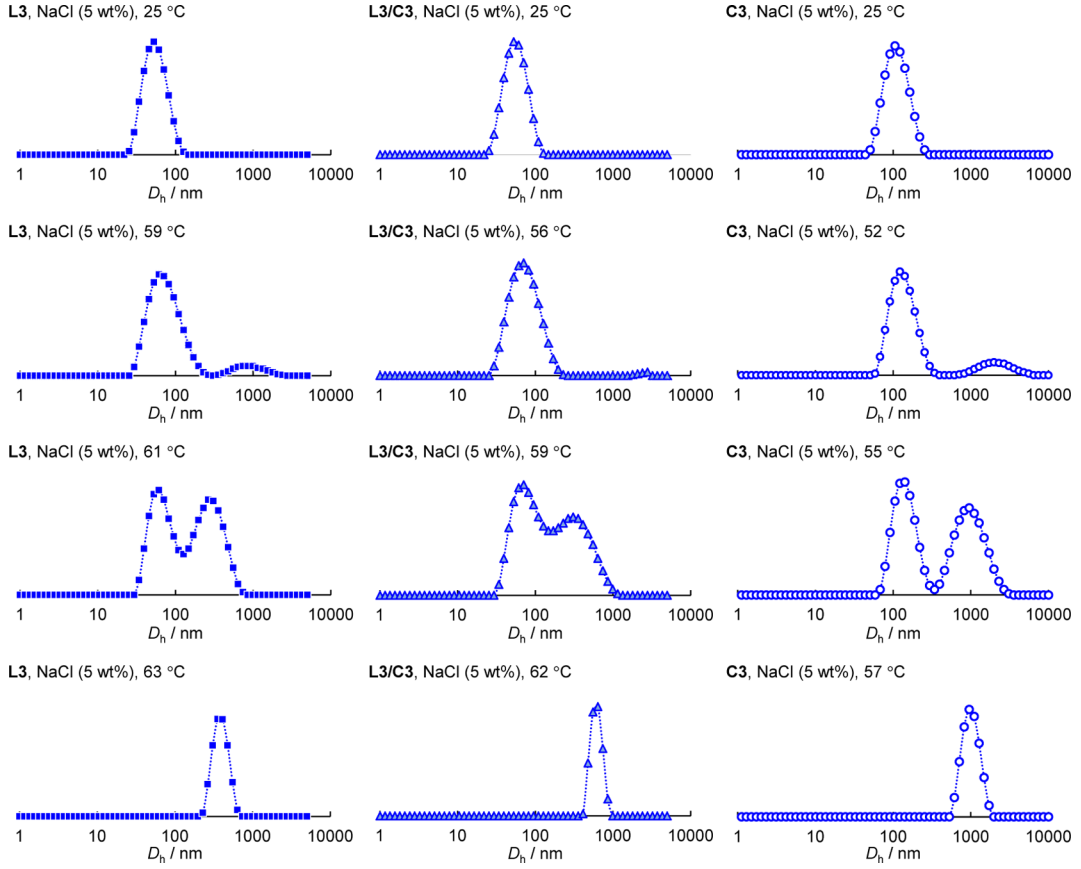

Figure 4. Temperature-dependent D_h distributions by number for vesicular solutions of **L3** (left), a one-to-one mixture of **L3**/**C3** (middle) and **C3** (right) in the presence of 5 wt % NaCl. Aggregates started to form at 59, 56, and 52 °C for **L3**, **L3**/**C3**, and **C3**, respectively.[46]

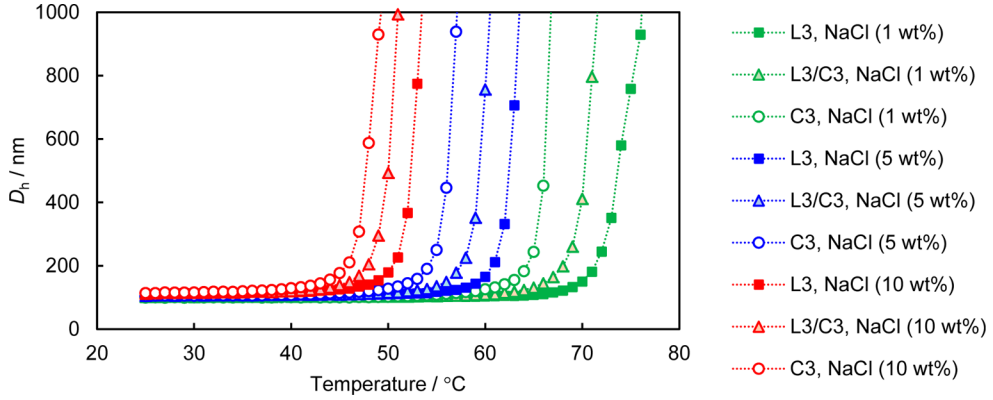

Figure 5. Temperature-dependent *z*-average diameter plots (1 °C step) for vesicular solutions of **L3**, a one-to-one mixture of **L3**/**C3**, and **C3** in the presence of NaCl (1, 5, and 10 wt %).[46]

decrease T_c by salting-out to evaluate potential differences in their thermal stability. Figure 4 shows the temperature-dependent D_h distributions for vesicular solutions of **L3** and **C3** in the presence of 5 wt % NaCl. Large particles (D_h > 150 nm) started to form at 59 °C for **L3**, and this temperature was defined as T_c. Upon agglomeration of the vesicles, a precipitate appeared. On the other hand, large particles appeared at 52 °C in the case of **C3**. Unlike the case of micelles from **L1** and **C1**, the formation of these large particles was irreversible, and thus, these large particles were expected to be agglomerates of disturbed vesicles. The *z*-average diameter of the vesicles was plotted against temperature in Figure 5. In the 5 wt % NaCl solutions of **L3** and **C3** vesicles, a sharp increase in the *z*-average diameter was observed at corresponding T_c. The thermal stability test was performed at different NaCl concentrations. In 1 wt % NaCl, vesicular solutions of **L3** and **C3** formed large particles at 69 and 62 °C, respectively (Figure S10). Moreover, T_c decreased to 48 and 43 °C in 10 wt % NaCl (Figure S11). The results are summarized in Table 2. In any cases, vesicles from the linear block copolymer showed higher thermal stability than the cyclic counterpart to some extent opposing to the case of the micelles.[24] These experiments were repeated to confirm the reproducibility of the relative thermal stability of the vesicles using different batches of self-assembly (Figures S12 and S13). Although each T_c differed by a few degrees by batches, the trend of T_c(**C3**) <

DOI: 10.1021/acs.langmuir.6b03148
Langmuir 2016, 32, 10344−10349

Table 2. T_c of Vesicles from L3, a One-to-One Mixture of L3/C3 and C3 in the Presence of 1, 5, and 10 wt % NaCl

NaCl (wt %)	L3 (°C)	L3/C3 (one-to-one) (°C)	C3 (°C)
1	69	66	62
5	59	56	52
10	48	46	43

T_c(**L3**) was consistent. Moreover, we attempted to control T_c by mixing a one-to-one ratio of the linear and cyclic copolymers (**L3**/**C3**) as previously reported for the micelles.[23,24] In the results, T_c was successfully tuned to the approximate midst of those of the vesicles from **L3** and **C3** in all the NaCl concentrations (Figures 4, 5, S10, and S11, Table 2).

We consider that this difference in the thermal stability is because of packing of the bilayer especially at the hydrophobic chains. By cyclization of the block copolymer, the bilayer structure is disturbed to some degree likely due to the bent conformation of the polymer chain. Concerning thermophilic archaea, the cell membrane is not constructed only with cyclic lipids. It also includes various proteins, cholesterol, and so on as well as double-tailed lipids and tetraether lipids with two head groups.[22] Thus, the above results show that the cyclic topology of the amphiphile is not a unique factor to determine the vesicles' thermal stability. Interactions with other substances in the cell membrane are also essential. Nevertheless, the topology of the amphiphile is indeed one of the novel approaches to control the properties of self-assembled entities for the production of new functional materials.

In the meantime, for the construction of vesicles, we initially employed linear poly(*n*-butyl acrylate)−poly(ethylene oxide)−poly(*n*-butyl acrylate) and cyclic poly(*n*-butyl acrylate)−poly(ethylene oxide), which were previously used for the formation of flower-like micelles.[23,24] However, no matter what segment ratio and self-assembly method were attempted, a precipitate formed, and no selective formation of vesicles was attained. This was likely due to the glass transition temperature (T_g) of the hydrophobic segments that would form the inner layer of the bilayer structure. Because poly(*n*-butyl acrylate) is in a rubbery state at ambient temperature (T_g = −49 °C),[45] a sufficiently robust inner layer cannot not be constructed. On the other hand, PS has T_g at 100 °C and is in a glassy state under the experimental temperatures, likely allowing for the formation of a robust inner layer. Presumably, the use of PS segment was the successful cause to construct the vesicles.

CONCLUSIONS

Self-assembled structures were investigated by varying the volume fractions of the hydrophilic and hydrophobic segments of cyclic block copolymers. Based on the molecular weight of the PS segment, the self-assembled structure was micelles, large compound micelles, or vesicles. The successfully constructed vesicles from the cyclic amphiphilic block copolymer may serve as a model for the cell membrane of thermophilic archaea. However, the vesicles from cyclic amphiphiles were actually less thermally stable than the linear counterparts. These results provide insights into the role of other substances existing in the lipid bilayer such as proteins and cholesterol for the significant thermal stability.

ASSOCIATED CONTENT

Supporting Information

The Supporting Information is available free of charge on the ACS Publications website at DOI: 10.1021/acs.langmuir.6b03148.

^{1}H NMR spectra, SEC traces, D_h distributions, temperature-dependent transmittance plots, photographs, TEM images, and Debye plots, temperature-dependent *z*-average diameter plots. (PDF)

AUTHOR INFORMATION

Corresponding Author

*E-mail: yamamoto.t@eng.hokudai.ac.jp.

Present Address

§Department of Industrial Chemistry, Faculty of Engineering, Tokyo University of Science, 12−1 Ichigaya-Funagawara-Machi, Shinjuku-Ku, Tokyo 162−0826, Japan.

Notes

The authors declare no competing financial interest.

ACKNOWLEDGMENTS

The authors are grateful to Prof. M. Kakimoto for access to measurement facilities. We thank the Center for Advanced Materials Analysis, Tokyo Institute of Technology for TEM observations. This work was supported by KAKENHI (26288099 T.Y., 15H01595 T.Y., and 15K13703 T.Y.).

REFERENCES

(1) Yamamoto, T.; Tezuka, Y. Cyclic polymers revealing topology effects upon self-assemblies, dynamics and responses. *Soft Matter* **2015**, *11*, 7458−7468.

(2) Bielawski, C. W.; Benitez, D.; Grubbs, R. H. An "endless" route to cyclic polymers. *Science* **2002**, *297*, 2041−2044.

(3) Tezuka, Y.; Ohtsuka, T.; Adachi, K.; Komiya, R.; Ohno, N.; Okui, N. A defect-free ring polymer: Size-controlled cyclic poly(tetrahydrofuran) consisting exclusively of the monomer unit. *Macromol. Rapid Commun.* **2008**, *29*, 1237−1241.

(4) Kitahara, T.; Yamazaki, S.; Kimura, K. Effects of topological constraint and knot entanglement on the crystal growth of polymers proved by growth rate of spherulite of cyclic polyethylene. *Kobunshi Ronbunshu* **2011**, *68*, 694−701.

(5) Su, H.-H.; Chen, H.-L.; Díaz, A.; Casas, M. T.; Puiggalí, J.; Hoskins, J. N.; Grayson, S. M.; Pérez, R. A.; Müller, A. J. New insights on the crystallization and melting of cyclic PCL chains on the basis of a modified Thomson-Gibbs equation. *Polymer* **2013**, *54*, 846−859.

(6) Habuchi, S.; Fujiwara, S.; Yamamoto, T.; Tezuka, Y. Single-molecule imaging reveals topological isomer-dependent diffusion by 4-armed star and dicyclic 8-shaped polymers. *Polym. Chem.* **2015**, *6*, 4109−4115.

(7) Doi, Y.; Matsubara, K.; Ohta, Y.; Nakano, T.; Kawaguchi, D.; Takahashi, Y.; Takano, A.; Matsushita, Y. Melt rheology of ring polystyrenes with ultrahigh purity. *Macromolecules* **2015**, *48*, 3140−3147.

(8) Zhang, K.; Lackey, M. A.; Cui, J.; Tew, G. N. Gels based on cyclic polymers. *J. Am. Chem. Soc.* **2011**, *133*, 4140−4148.

(9) Hoskins, J. N.; Grayson, S. M. Synthesis and degradation behavior of cyclic poly(ε-caprolactone). *Macromolecules* **2009**, *42*, 6406−6413.

(10) Nasongkla, N.; Chen, B.; Macaraeg, N.; Fox, M. E.; Fréchet, J. M. J.; Szoka, F. C. Dependence of pharmacokinetics and biodistribution on polymer architecture: Effect of cyclic versus linear polymers. *J. Am. Chem. Soc.* **2009**, *131*, 3842−3843.

(11) Wei, H.; Chu, D. S. H.; Zhao, J.; Pahang, J. A.; Pun, S. H. Synthesis and evaluation of cyclic cationic polymers for nucleic acid delivery. *ACS Macro Lett.* **2013**, *2*, 1047−1050.

DOI: 10.1021/acs.langmuir.6b03148
Langmuir 2016, 32, 10344−10349

(12) Poelma, J. E.; Ono, K.; Miyajima, D.; Aida, T.; Satoh, K.; Hawker, C. J. Cyclic block copolymers for controlling feature sizes in block copolymer lithography. *ACS Nano* **2012**, *6*, 10845−10854.
(13) Endo, K. Synthesis and properties of cyclic polymers. *Adv. Polym. Sci.* **2008**, *217*, 121−183.
(14) Kricheldorf, H. R. Cyclic polymers: Synthetic strategies and physical properties. *J. Polym. Sci., Part A: Polym. Chem.* **2010**, *48*, 251−284.
(15) Hoskins, J. N.; Grayson, S. M. Cyclic polyesters: Synthetic approaches and potential applications. *Polym. Chem.* **2011**, *2*, 289−299.
(16) Jia, Z.; Monteiro, M. J. Cyclic polymers: Methods and strategies. *J. Polym. Sci., Part A: Polym. Chem.* **2012**, *50*, 2085−2097.
(17) Zhang, K.; Tew, G. N. Cyclic polymers as a building block for cyclic brush polymers and gels. *React. Funct. Polym.* **2014**, *80*, 40−47.
(18) Fiers, W.; Sinsheimer, R. L. The structure of the DNA of bacteriophage φX174: III. Ultracentrifugal evidence for a ring structure. *J. Mol. Biol.* **1962**, *5*, 424−434.
(19) Wikoff, W. R.; Liljas, L.; Duda, R. L.; Tsuruta, H.; Hendrix, R. W.; Johnson, J. E. Topologically linked protein rings in the bacteriophage HK97 capsid. *Science* **2000**, *289*, 2129−2133.
(20) Gessler, K.; Uson, I.; Takaha, T.; Krauss, N.; Smith, S. M.; Okada, S.; Sheldrick, G. M.; Saenger, W. V-amylose at atomic resolution: X-ray structure of a cycloamylose with 26 glucose residues (cyclomaltohexaicosaose). *Proc. Natl. Acad. Sci. U. S. A.* **1999**, *96*, 4246−4251.
(21) Yamagishi, A. Thermophiles and life science in space. *Biol. Sci. Space* **2000**, *14*, 332−340.
(22) Arakawa, K.; Eguchi, T.; Kakinuma, K. 36-Membered macrocyclic diether lipid is advantageous for archaea to thrive under the extreme thermal environments. *Bull. Chem. Soc. Jpn.* **2001**, *74*, 347−356.
(23) Honda, S.; Yamamoto, T.; Tezuka, Y. Topology-directed control on thermal stability: Micelles formed from linear and cyclized amphiphilic block copolymers. *J. Am. Chem. Soc.* **2010**, *132*, 10251−10253.
(24) Honda, S.; Yamamoto, T.; Tezuka, Y. Tuneable enhancement of the salt and thermal stability of polymeric micelles by cyclized amphiphiles. *Nat. Commun.* **2013**, *4*, 1574.
(25) Mai, Y.; Eisenberg, A. Self-assembly of block copolymers. *Chem. Soc. Rev.* **2012**, *41*, 5969−5985.
(26) Baba, E.; Honda, S.; Yamamoto, T.; Tezuka, Y. ATRP−RCM polymer cyclization: Synthesis of amphiphilic cyclic polystyrene-*b*-poly(ethylene oxide) copolymers. *Polym. Chem.* **2012**, *3*, 1903−1909.
(27) Hayashi, S.; Adachi, K.; Tezuka, Y. ATRP−RCM synthesis of 8-shaped poly(methyl acrylate) using a 4-armed star telechelics. *Polym. J.* **2008**, *40*, 572−576.
(28) Yu, K.; Zhang, L.; Eisenberg, A. Novel morphologies of "crew-cut" aggregates of amphiphilic diblock copolymers in dilute solution. *Langmuir* **1996**, *12*, 5980−5984.
(29) Cameron, N. S.; Corbierre, M. K.; Eisenberg, A. Asymmetric amphiphilic block copolymers in solution: a morphological wonderland. *Can. J. Chem.* **1999**, *77*, 1311−1326.
(30) Hayashi, S.; Adachi, K.; Tezuka, Y. An efficient route to cyclic polymers by ATRP−RCM process. *Chem. Lett.* **2007**, *36*, 982−983.
(31) Adachi, K.; Honda, S.; Hayashi, S.; Tezuka, Y. ATRP−RCM synthesis of cyclic diblock copolymers. *Macromolecules* **2008**, *41*, 7898−7903.
(32) Lawson, C. L.; Hanson, R. J. *Solving Least Squares Problems*; Prentice-Hall: Englewood Cliffs, NJ, 1974.
(33) Grabowski, E. F.; Morrison, I. D. In *Measurement of Suspended Particles by Quasi-Elastic Light Scattering*; Dahneke, B. E., Ed.; Wiley: New York, 1983.
(34) Morrison, I. D.; Grabowski, E. F.; Herb, C. A. Improved techniques for particle size determination by quasi-elastic light scattering. *Langmuir* **1985**, *1*, 496−501.
(35) Bryant, G.; Thomas, J. C. Improved particle size distribution measurements using multiangle dynamic light scattering. *Langmuir* **1995**, *11*, 2480−2485.
(36) Yuan, J.; Li, Y.; Li, X.; Cheng, S.; Jiang, L.; Feng, L.; Fan, Z. The "crew-cut" aggregates of polystyrene-*b*-poly(ethylene oxide)-*b*-polystyrene triblock copolymers in aqueous media. *Eur. Polym. J.* **2003**, *39*, 767−776.
(37) Bhargava, P.; Tu, Y.; Zheng, J. X.; Xiong, H.; Quirk, R. P.; Cheng, S. Z. D. Temperature-induced reversible morphological changes of polystyrene-*block*-poly(ethylene oxide) micelles in solution. *J. Am. Chem. Soc.* **2007**, *129*, 1113−1121.
(38) Israelachvili, J. N.; Mitchell, D. J.; Ninham, B. W. Theory of self-assembly of hydrocarbon amphiphiles into micelles. *J. Chem. Soc., Faraday Trans. 2* **1976**, *72*, 1525−1568.
(39) Israelachvili, J. The science and applications of emulsions − An overview. *Colloids Surf., A* **1994**, *91*, 1−8.
(40) Zhang, L.; Eisenberg, A. Multiple morphologies and characteristics of "crew-cut" micelle-like aggregates of polystyrene-*b*-poly(acrylic acid) diblock copolymers in aqueous solutions. *J. Am. Chem. Soc.* **1996**, *118*, 3168−3181.
(41) Yu, Y.; Zhang, L.; Eisenberg, A. Morphogenic effect of solvent on crew-cut aggregates of apmphiphilic diblock copolymers. *Macromolecules* **1998**, *31*, 1144−1154.
(42) Annable, T.; Buscall, R.; Ettelaie, R.; Whittlestone, D. The rheology of solutions of associating polymers: Comparison of experimental behavior with transient network theory. *J. Rheol.* **1993**, *37*, 695−726.
(43) Semenov, A. N.; Joanny, J. F.; Khokhlov, A. R. Associating polymers: equilibrium and linear viscoelasticity. *Macromolecules* **1995**, *28*, 1066−1075.
(44) Pham, Q. T.; Russel, W. B.; Thibeault, J. C.; Lau, W. Micellar solutions of associative triblock copolymers: Entropic attraction and gas−liquid transition. *Macromolecules* **1999**, *32*, 2996−3005.
(45) *Polymer Handbook*; Brandrup, J., Immergut, E. H., Eds.; Wiley: New York, 1989.
(46) In Figures 3−5, S3, S4, S7, S9−S13, the following symbols and colors are applied: square, **L1**, **L2**, and **L3**; circle, **C1**, **C2**, and **C3**; black, 0 wt% NaCl solution; green, 1 wt% NaCl solution; blue, 5 wt% NaCl solution; red, 10 wt% NaCl solution.

DOI: 10.1021/acs.langmuir.6b03148
Langmuir 2016, 32, 10344−10349